Size and anisotropy effects on static and dynamic properties of ferromagnetic nanoparticles

2007 J. Phys.: Condens. Matter 19 216208

(http://iopscience.iop.org/0953-8984/19/21/216208)

IOP PUBLISHING JOURNAL OF PHYSICS: CONDENSED MATTER

J. Phys.: Condens. Matter **19** (2007) 216208 (13pp) doi:10.1088/0953-8984/19/21/216208

Size and anisotropy effects on static and dynamic properties of ferromagnetic nanoparticles

J M Wesselinowa[1] **and I Apostolova**[2]

[1] Department of Physics, University of Sofia, Boulevard J Bouchier 5, 1164 Sofia, Bulgaria
[2] Faculty of Forest Industry, Univeristy of Forestry, 10 Kliment Okhridsky Boulevard, 1756 Sofia, Bulgaria

Received 19 January 2007, in final form 5 April 2007
Published 27 April 2007
Online at stacks.iop.org/JPhysCM/19/216208

Abstract

Based on the modified Heisenberg model we analyse the influence of size and anisotropy effects on static and dynamic properties of ferromagnetic nanoparticles. A Green's function technique in real space enables us to calculate the excitation energy and its damping as well as the magnetization depending on the temperature and the size of the particles. The critical temperature is also determined by the size of the particles. With decreasing particle size the spin-excitation energy can decrease or increase for different surface exchange interaction constants, whereas the damping always increases. Additionally, we consider the influence of surface anisotropy and external magnetic field on the excitation spectrum. The theoretical results are in reasonable accordance with experimental data.

1. Introduction

Magnetic nanoparticles show a variety of unusual magnetic behaviours when compared to the bulk materials, mostly due to finite size effects, surface/interface effects, including symmetry breaking, electronic environment/charge transfer and magnetic interactions. Magnetic properties such as magnetization, hysteresis and phase transition temperature show reasonable size dependences. They are found to be reduced [1–4] or enhanced [5–7] in small particles due to surface spin disorder. High-frequency collective magnetic excitations in magnetic nanoparticles are obtained from neutron scattering experiments [8, 9]. These excitations include discretized spin wave modes and surface modes [10]. Recent experiments revealed particle size scaling laws in the resonance peak frequency dependence in Co–Ni nanoparticles [11]. A theoretical analysis of these experiments has been made by Ferchmin [12]. X-ray diffraction measurements have been performed on $LaSrMnO_3$ nanoparticles by Roy *et al* [13]. Collective excitations are observed, but due to finite size effects they do not follow the Bloch law. Respaud *et al* [14] reported on high-frequency ferromagnetic resonance measurements on ultrafine Co particles with strong uniaxial effective anisotropy. The transverse relaxation

time is two orders of magnitude smaller than the bulk value, indicating strong damping effects, possible originating from surface spin disorder. Single-electron tunnelling spectroscopy studies [15, 16] have succeeded in resolving the excitation spectra of ferromagnetic transition-metal nanoparticles. The discrete resonances seen in the tunnelling experiments measure the low-energy many-electron excitation spectra of a single-domain ferromagnetic nanoparticle. X-ray diffraction measurements were performed to study the static and dynamic magnetic properties of spherical magnetite [1] and of $SnFe_2O_4$ nanoparticles [2]. It was found that the width of the diffraction peaks increases as the size of the nanoparticles decreases. Sanchez *et al* [3] and Hsu *et al* [17] presented magnetic resonance experiments in order to study the dynamic behaviours of resonance field and resonance linewidth for $Y_3Fe_5O_{12}$ and Fe_3O_4 nanoparticles with different sizes, respectively. The superparamagnetic effects in the ferromagnetic resonance of Ni particles are investigated by Sharma and Baiker [18]. Broadening of the resonance occurs at lower temperatures. The anisotropy field is reduced in the particles as compared to bulk Ni. Concurrently with the line broadening, the resonance shifts to lower magnetic fields. By use of inelastic neutron scattering, Kuhn *et al* [19] have studied magnetic fluctuations in 8 nm haematite nanoparticles as a function of temperature and applied magnetic fields. They observed an increase in the width of the inelastic peak with increasing temperature, which is correlated to the excessive magnetic dynamics such as $q = 0$ spin waves within the particles. For the interacting nanoparticles the width is a factor of two to three larger, indicating that there is a broad range of interaction energies.

Whereas the static properties of small metal particles or clusters can be obtained at a microscopic level, the situation is much worse as far as the dynamical properties are concerned, because the Monte Carlo studies did not describe the detailed dynamical behaviour. The spin-wave spectrum of Heisenberg spin clusters of various structures ranging in size between 9 and 749 spins is calculated by a self-consistent diagonalization of the equation of motion of S^+ in real space by Hendriksen *et al* [20]. The spin-wave spectrum of the clusters is strongly modified relative to the bulk. The anisotropy effects are not taken into account. Canali and MacDonald [21] reported a theory of the low-energy excitations of a ferromagnetic metal nanoparticle. In addition to the particle–hole excitations, which occur in a paramagnetic metal nanoparticle, they predicted a branch of excitations involving the magnetization-orientation collective coordinate. A theoretical treatment of spin-wave excitations in ferromagnetic wires and particles in the presence of single-ion surface anisotropy is developed within the framework of the matrix theory by Ferchmin and Puszkarski [22]. Recently, Cehovin *et al* [23] have presented a theory of the elementary spin excitations in transition-metal ferromagnet nanoparticles which achieves a unified and consistent quantum description of both collective and quasiparticle physics. Arias *et al* [24] presented explicit calculations of the mode spectrum of a ferromagnetic sphere, along with the response functions which describe excitation of spin wave modes by spatially inhomogeneous fields. Using a spin-wave model Morup and Hansen [25] have shown that the uniform precession mode, corresponding to a spin wave with wavevector $q = 0$, is predominant in nanoparticles. This is in accordance with the results of a classical model for collective magnetic excitations in nanoparticles [26]. Shilov *et al* have presented a macroscopic model of the effect of uniaxial surface anisotropy [27] and unidirectional surface anisotropy [28] on the magnetodynamics of ferrite nanoparticles using the Landau–Lifshitz equation. It is shown that in the first case the surface can produce a considerable shift of the precession frequency whereas in the second case the surface effect is equivalent to the presence of an additional intrinsic size-dependent field coaligned with the constant magnetizing one. This model is most appropriate at low temperatures. In all previous papers the linewidth of the resonance peaks is not considered. Recently, the dynamical response of nanoparticles as probed by ferromagnetic resonance has been studied by Usadel [29] within

a classical spin model using Landau–Lifshitz–Gilbert dynamics. The dependence of both the shift of the resonance signal and the linewidth on temperature is obtained.

The aim of the present paper is to study the size and anisotropy effects on the static and dynamic properties of magnetic nanoparticles including single-ion anisotropy using a Green's function theory in order to explain the different experimental and theoretical results.

2. The model and the matrix Green's function

In this section we present calculations for obtaining the spin Green's function for a ferromagnetic nanoparticle. This method seems still probably the most appropriate tool to study complex systems with low symmetry. Different to extended materials, the Green's function for small particles has to be formulated in real space [22]. Moreover, the real-space Green's function leads directly to the local density of states. Because of the presence of, at most, only partial long-range order and, in many cases, the complete absence of long-range order, such a nanoparticle is nevertheless sufficiently complex and involves usually a large number of relevant degrees of freedom. Therefore, the calculation of the real-space Green's function of such a complex system is a formidable task. A nanoparticle is defined by fixing the origin of a certain spin in the centre of the particle and including all spins within the particle in shells. The shells are numbered by $n = 1, \ldots, N$, where $n = 1$ denotes the central spin and $n = N$ represents the surface shell of the system. The exchange interaction between nearest-neighbour spins is modelled using the Heisenberg model including single-site uniaxial anisotropy,

$$H = -\sum_{i,j} J_{ij}(S_i^+ S_j^- + S_i^z S_j^z) - \sum_i D_i (S_i^z)^2 - g\mu_B H \sum_i S_i^z, \tag{1}$$

where S_i^+, S_i^- and S_i^z are the spin operators for the localized spins of the atom at site i in the particle, J_{ij} is the exchange interaction and $D_i (D < 0)$ is the single-site anisotropy parameter, $|D| < J$. H is an external magnetic field. We assume for simplicity only nearest-neighbour exchange interaction and take $J_{ij} = J_s$, $D_i = D_s$ on the surface of the particle and $J_{ij} = J_b$, $D_i = D_b$ in the particle. It is important to mention that the exchange interaction $J_{ij} = J(r_i - r_j)$ depends on the distance between the spins, i.e. on the lattice parameter, on the lattice symmetry and on the number of next nearest neighbours. This is very important for investigations of ion doping effects. The critical temperatures are connected with the exchange interaction constants. They can be calculated from the relation $T_C = JzS(S+1)/3k_B$, where z is the number of nearest neighbours, S the spin value and k_B the Boltzmann constant. From this relation we have obtained the exchange interaction constant of the bulk Fe with bcc lattice where $T_C = 1043$ K, $z = 8$ and $S = 2$ to $J_b = 64,77$ K.

Macroscopic and microscopic quantities can be calculated by using the retarded Green's function, which is defined as

$$G_{ij}(t) = -\mathrm{i}\theta(t)\langle [S_i^+(t); S_j^-]\rangle. \tag{2}$$

After a formal integration of the equation of motion for (2), one obtains [30]

$$G_{ij}(t) = -\mathrm{i}\theta(t)\langle [S_i^+; S_j^-]\rangle \exp(-\mathrm{i}E_{ij}(t)t) \tag{3}$$

where

$$E_{ij}(t) = E_{ij} - \frac{\mathrm{i}}{t}\int_0^t \mathrm{d}t' t' \left(\frac{\langle [j_i(t); j_j^+(t')]\rangle}{\langle [S_i^+(t); S_j^-(t')]\rangle} - \frac{\langle [j_i(t); S_j^-(t')]\rangle \langle [S_i^+(t); j_j^+(t')]\rangle}{\langle [S_i^+(t); S_j^-(t')]\rangle^2} \right) \tag{4}$$

with the notation $j_i(t) = \langle [S_i^+, H_{\mathrm{int}}]\rangle$. The time-independent term

$$E_{ij} = \frac{\langle [[S_i^+, H]; S_j^-]\rangle}{\langle [S_i^+; S_j^-]\rangle} \tag{5}$$

is the spin-excitation energy in the generalized Hartree–Fock approximation (GHFA). The time-dependent term in equation (5) includes damping effects.

For the spin-excitation energies we obtain the following expression in the GHFA:

$$E_{ij} = \left(\frac{2}{N}\sum_m J_{im}(\langle S_m^- S_i^+\rangle + 2\langle S_m^z S_i^z\rangle)\delta_{ij} - 2J_{ij}(\langle S_i^- S_j^+\rangle + 2\langle S_i^z S_j^z\rangle) + 2D_i(2\langle S_i^z S_i^z\rangle - \langle S_i^- S_i^+\rangle)\delta_{ij} + 2g\mu_B H\langle S_i^z\rangle\delta_{ij}\right) \Big/ 2\langle S_i^z\rangle\delta_{ij}. \quad (6)$$

If we neglect the transverse correlation functions $\langle S_i^- S_j^+\rangle$ and decouple the longitudinal correlation functions $\langle S_i^z S_j^z\rangle \rightarrow \langle S_i^z\rangle\langle S_j^z\rangle$ we obtain E in the random phase approximation (RPA),

$$E_{ij} = g\mu_B H\delta_{ij} + \frac{2}{N}\sum_m J_{im}\langle S_m^z\rangle\delta_{ij} - 2J_{ij}\langle S_i^z\rangle + 2D_i\langle S_i^z\rangle\delta_{ij}. \quad (7)$$

The experimentally obtained large width at half-maximum in the resonance spectra cannot be understood within the RPA for small particles. Using the method of Tserkovnikov [30] we go beyond the RPA and calculate the damping of the spin excitations in ferromagnetic particles in the GHFA to be

$$\gamma_{ss}(i) = \frac{4\pi}{N}\sum_l J_{il}^2 M_i M_l[\bar{n}_l(1+\bar{n}_l+\bar{n}_i) - \bar{n}_l\bar{n}_i]\delta(E_l + E_i - E_i - E_l) + 2\pi D_i^2 M_i^2\bar{n}_i(1+\bar{n}_i)\delta(E_i - E_i), \quad (8)$$

where $\bar{n}_m = \langle S_m^- S_m^+\rangle$ is the correlation function calculated from the spectral theorem.

3. Numerical results and discussion

In this section we present the numerical calculations of our theoretical results for a spherical magnetic nanoparticle taking the following model parameters appropriate for Fe: $J_b = 60$ K, $D_b = -20$ K, $S = 2$. Due to the changed number of next nearest neighbours on the surface, the interaction constant J can take different values for the surface J_s compared to the value in the particle J_b. Firstly we present the temperature dependence of the average magnetization and the average spin excitation energy for different values of the surface exchange interaction constant J_s in figures 1 and 2. For the case where the exchange interaction of the surface shell takes the value $J_s = 0.1J_b$ (figure 1, curve 1), i.e. J_s is smaller than the value of the exchange interaction constant in the particle J_b, the average magnetization (respectively the spin excitation energy—figure 2) is reduced compared to the case for $J_s = J_b$ (curve 2). The magnetization and the spin modes decrease with increasing temperature and vanish at the critical temperature T_C of the particle in accordance with the experimental data of Pishko *et al* [31] and Winkler *et al* [32]. The critical temperature decreases due to the smaller value of the surface-coupling J_s. In the case $J_s = 3J_b$, i.e. $J_s > J_b$ (figure 1, curve 3) the average magnetization (respectively the spin excitation energy—figure 2) is larger compared to the case $J_s = J_b$ (curve 2). The critical temperature T_C of the small particle is enhanced due to the presence of larger J_s values. This behaviour is directly opposed to the case of $J_s < J_b$. In figure 3 we show the temperature dependence of the shell spin excitations for a particle with $N = 5$ shells and different J_s-values. We obtain analogous dependences for the shell magnetizations. It is demonstrated that for $J_s < J_b$ the spin excitation energy of the surface shell $n = 5$ (full line) is smaller compared with that of the central atom, $n = 1$ (full line), whereas for $J_s > J_b$ it becomes larger ($n = 5$, dashed line) than the spin excitation of the central atom ($n = 1$, dashed line). Experimental evidence of surface effects in the magnetic dynamics behaviour of ferrite nanoparticles is given by Sousa

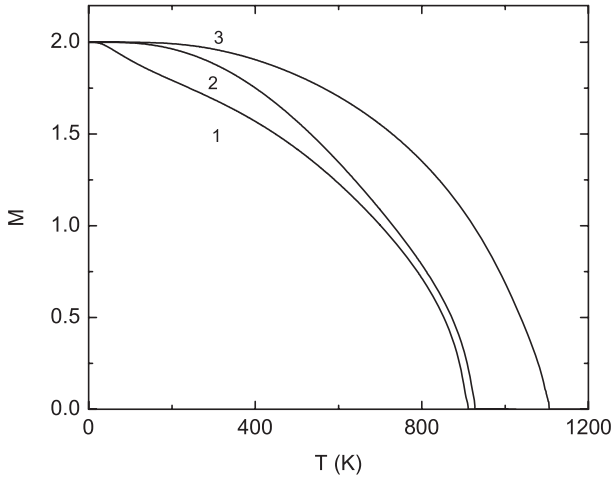

Figure 1. Temperature dependence of the average magnetization M for a spherical ferromagnetic particle for $N = 5$ shells, $D_s = D_b$, $H = 0$ and different J_s-values: (1) $J_s = 0.1J_b$, (2) $J_s = J_b$, (3) $J_s = 3J_b$.

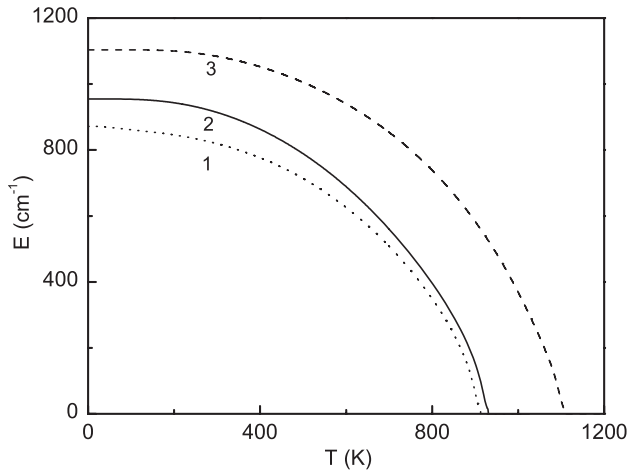

Figure 2. Temperature dependence of the average spin excitation energy E for a spherical ferromagnetic particle for $N = 5$ shells, $D_s = D_b$, $H = 0$ and different J_s-values: (1) $J_s = 0.1J_b$, (2) $J_s = J_b$, (3) $J_s = 3J_b$.

et al [33]. Such surface modes have been detected by quasielastic neutron scattering [10] and magnetic resonance experiments [11].

The damping γ corresponds to the full width at half-maximum (FWHM) of the resonance line. It seems to have been generally accepted that phase transitions in nanoparticles are 'wide' and not sharp as in the bulk due to the larger damping effects obtained in nanoparticles. We have calculated the spin excitation damping. The temperature dependence of γ for different values of the surface exchange interaction constant J_s is shown in figure 4. The damping increases with increasing J_s and increasing temperature. So, the larger damping effects cause a broadening of the resonance peaks at high temperatures. This is in accordance with the theoretical results of Usadel [29] and the experimental data of Kuhn *et al* [19] for α-Fe_2O_3 nanoparticles.

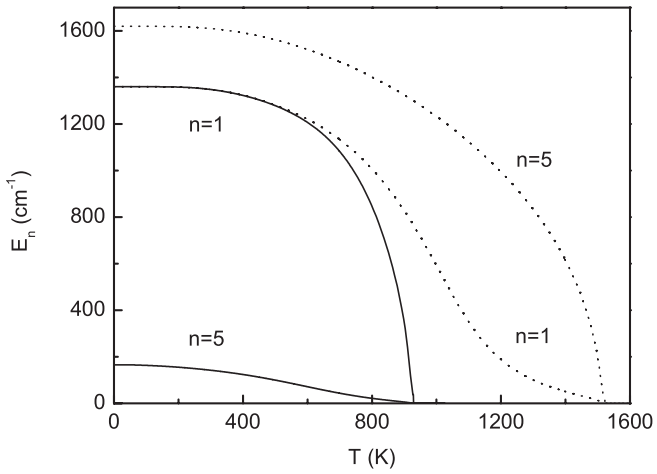

Figure 3. Temperature dependence of the shell spin excitation energy E_n for $N = 5$ shells, $D_s = D_b$, $H = 0$, $J_s = 4J_b$ (full curves), $J_s = 0.2J_b$ (dashed curves) and $n = 1$—central atom, $n = 5$—surface shell.

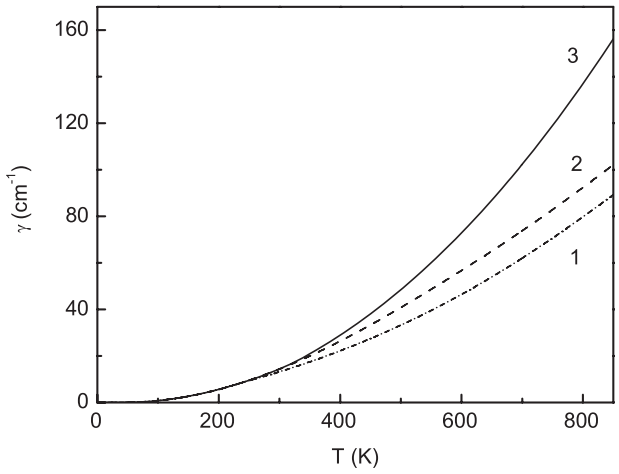

Figure 4. Temperature dependence of the spin excitation damping γ for $N = 5$ shells, $D_s = D_b$, $H = 0$ and different J_s-values: (1) $J_s = 0.2J_b$, (2) $J_s = J_b$ and (3) $J_s = 3J_b$.

At the same time there are some experimental data mainly in ferrite [17, 34–36] and antiferromagnetic [37, 38] nanoparticles which show that the resonance field H_r increases whereas the FWHM (γ) decreases with increasing temperature. De Biasi *et al* [39] have presented the results of ferromagnetic resonance measurements on noninteracting amorphous magnetic nanoparticle systems. They remarked the existence of two behaviours, one at low and the other at high temperature. The temperature dependence of the line width has a maximum and the resonance field has a minimum. In the high-temperature regime they observe a close to symmetric line shape with decreasing linewidth with increasing T and a superparamagnetic behaviour. At low temperatures the FMR behaviour shows signs of a high anisotropy and the line width decreases with decreasing T. Unfortunately, there are not so many experiments on the temperature dependence of the resonance field and linewidth in

ferromagnetic nanoparticles. But using the analogy between ferromagnetic and ferroelectric thin films or nanoparticles we can see that there are many experimental data in ferroelectric nanoparticles of $BaTiO_3$ [40], $PbTiO_3$ [41] and $BaSrTiO_3$ [42] in which it is observed that the energy decreases and the damping increases with increasing temperature, in accordance with our finding. It may be that these differences between the temperature dependences of H_r and the FWHM in ferromagnetic and ferri- or antiferromagnetic nanoparticles are due to the different magnetic exchange interactions. For example, in ferri- and antiferromagnetic systems a superexchange occurs via an oxygen atom. The antiferromagnetic nanoparticles have a nonzero magnetic moment in contrast to the bulk case, which has been attributed to uncompensated spins [43] or to a contribution from so-called thermoinduced magnetization [44]. Moreover, macroscopic quantum tunnelling of the magnetization, which is characterized by a temperature-independent relaxation, is expected to be more pronounced in antiferromagnetic nanoparticles than in ferromagnetic nanoparticles [45]. In order to obtain the properties in ferri- and antiferromagnetic nanoparticles we must extend our model, including two sublattices with different spin directions and spin values or even more, eight, six or four, sublattices [46]. Furthermore, the temperature dependence of the anisotropy must be taken into account. Thus, further theoretical studies and interpretations of the magnetic resonance experimental data of magnetic nanoparticles remain very important.

There is some experimental evidence that the magnetic anisotropy of nanoparticles can be larger [47, 48] or smaller [18, 49] than that of the bulk materials. A major contribution of this enhancement or reduction comes from the surface spins. Ferromagnetic resonance is a useful tool to probe the type and strength of the particle surface anisotropy. We have calculated numerically the magnetization M, the spin excitation E and the damping γ in dependence of D_s/D_b. The results are shown in figure 5. The spin excitation energy (figure 5, curves 1a, 1b) (and analogously the magnetization) decreases with increasing surface anisotropy values D_s, whereas the damping increases with increasing D_s (figure 5, curves 2a, 2b). We would mention that, for example, for the case $J_s > J_b$ (curve 2) with decreasing temperature the curve is steeper, i.e. we obtain stronger dependence on D_s/D_b. There is some competition between the influence of J_s, which enhances the magnetization M and the spin excitation energy E, and of D_s, which reduces them. Nevertheless, the FWHM of the resonance line (or γ) is expected to depend more strongly upon the comparison the surface-to-bulk anisotropy ratio (see for example [36, 50, 51]). In order to obtain stronger dependences we must take into account the temperature and size dependence of the single-ion anisotropy D_s, the exchange anisotropy and the dipole–dipole interactions between the particles, which is not considered here.

In order to study the size effects, the magnetization, the Curie temperature, the spin excitation energy and the damping for particles with different shell numbers are calculated numerically. The results are demonstrated in figures 6–10. The magnetization and the phase transition temperature can be enhanced or reduced in comparison to the bulk due to increasing or decreasing of the surface exchange interaction constant J_s. In order to understand that the moments increase or decrease with decreasing particle size, we have to consider two competing factors that determine the magnetic moments in small particles. The decreasing coordination number in small particles tends to enhance the moment. On the other hand, the interatomic distances in metallic particles increase as particles grow in size. This factor would tend to lower the particle moments as their size gets smaller. The particle size dependences of the magnetization M and T_C for $D_s/D_b = \text{const}$ and different J_s/J_b-values are presented in figures 6 and 7. There is a critical value of $N_{cr} = 3$ shells below which there cannot exist a ferromagnetic phase. Below N_{cr} we have superparamagnetism. The first case $J_s < J_b$ (figures 6, 7—curve 1) could explain the experimental data of decrease of the magnetization M and the phase transition temperature T_C in small particles of magnetite [1], $SnFe_2O_4$ [2],

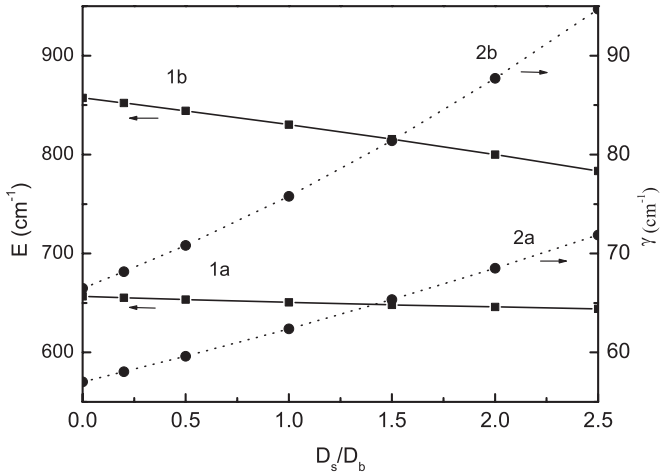

Figure 5. Dependence of the average spin excitation energy E (curves 1) and the damping γ (curves 2) on the surface anisotropy D_s/D_b for $N = 5$ shells, $T = 600$ K and different J_s-values: (a) $J_s = 0.2J_b$ and (b) $J_s = 2J_b$.

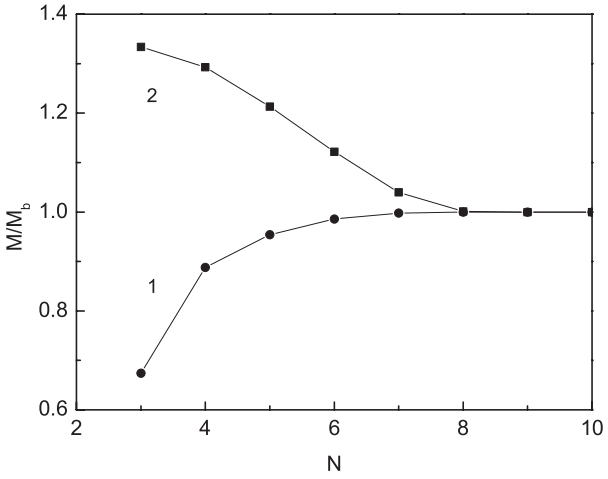

Figure 6. Particle size dependence of the magnetization M/M_b for $D_s = D_b$, $T = 700$ K and different J_s-values: (1) $J_s = 0.2J_b$ and (2) $J_s = 3J_b$.

$Y_3Fe_5O_{12}$ [3], Ni and Co [4]. The second case $J_s > J_b$ (figures 6, 7—curve 2) is responsible for example for the enhancement of M and T_C in Co [5] and ferrite nanoparticles [6]. There exists a critical value J_{sc}, below which the particle can be magnetically ordered only as a whole. However, for $J_s > J_{sc} = 1.22$–1.23 J_b (for $D_s/D_b = 1$) a surface ferromagnetic phase is possible. This critical value J_{sc} depends on the surface anisotropy. For example, for $D_s/D_b = 0.1$ it is 1.30, i.e. it is enhanced for reduced D_s-values.

We have seen from figure 5 that the physical properties depend on the surface single-ion anisotropy constant D_s. It must be noted that for the case $J_s > J_b$, for example $J_s = 2J_b$, and strong surface anisotropy, for example $D_s/D_b = 2$, the magnetization is larger compared to the bulk value and the curve in the size dependence of the magnetization $M(N)$ has a maximum at low particle size, $n = 4$ (figure 8, curves 1 and 3). For small surface anisotropy,

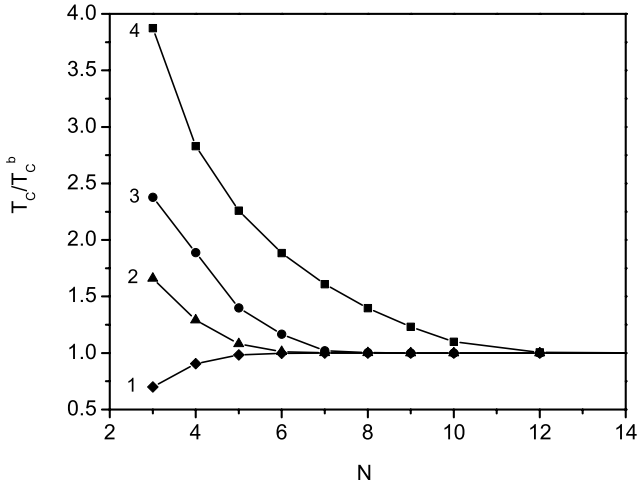

Figure 7. Particle size dependence of the phase transition temperature T_C/T_C^b for $D_s = D_b$ and different J_s-values: (1) $J_s/J_b = 0.2$, (2) 2, (3) 3 and (4) 5.

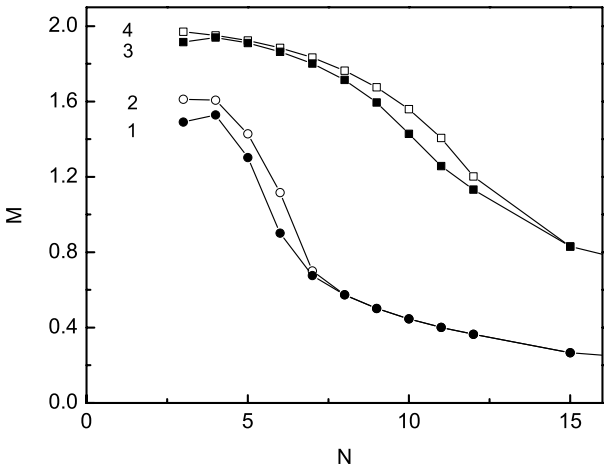

Figure 8. Particle size dependence of the magnetization M for $J_s = 2J_b$ and different temperatures T and different D_s-values: (1) $D_s = 2D_b$, $T = 800$ K; (2) $D_s = 0.2D_b$, $T = 800$ K, (3) $D_s = 2D_b$, $T = 400$ K; (4) $D_s = 0.2D_b$, $T = 400$ K.

$D_s < D_b$, (figure 8, curves 2 and 4) the magnetization M decreases with increasing particle size N; there is no maximum. A similar maximum is obtained in the dependence $E(N)$ for $J_s/J_b = 2$ and $D_s/D_b = 2$, too. The maximum decreases with decreasing temperature. The magnetization at high temperatures decreases more steeply with increasing particle size. Such a maximum in $M(N)$ is observed in Au nanoparticles by Hori *et al* [7]. A similar maximum in H_c at diameters of ≈10–20 nm is obtained experimentally due to strong surface anisotropy for example in spherical Co–Ni and Fe–Co–Ni particles [11], yttrium iron garnet nanoparticles [52] and $CoFe_2O_4$ nanoparticles [53]. We can conclude that the magnetic single-ion anisotropy, and mainly the surface anisotropy, plays a dominant role in determining the magnetic properties of particles and must be taken into account in order to explain the experimental data.

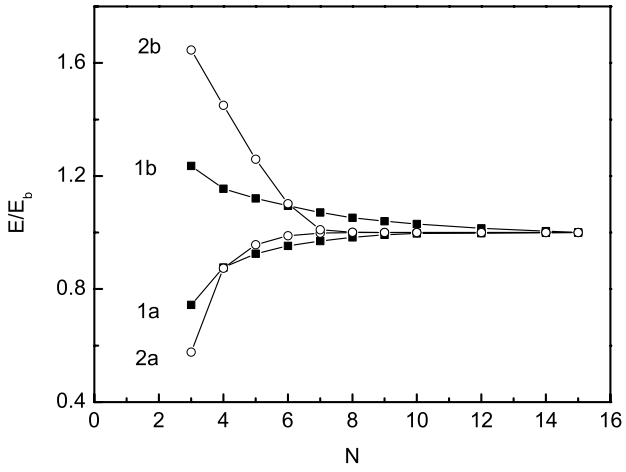

Figure 9. Particle size dependence of the spin excitation energy E/E_b for different temperatures T, (1) $T = 400$ K and (2) $T = 700$ K, and different J_s-values: (a) $J_s = 0.2J_b$ and (b) $J_s = 2J_b$.

The observed increasing or decreasing of the spin excitations with decreasing particle size (figure 9) due to different surface effects is in accordance with different experimental data. The spin energy curve is steeper for the case $J_s < J_b$. It can be seen from figure 9 that reaching the bulk energy value is dependent on the temperature. At high temperatures E_b is reached for smaller particles. The spin excitation energy E decreases strongly with increasing particle size for $J_s > J_b$ at high temperatures. For $J_s < J_b$ the spin excitation energy E decreases with decreasing particle sizes (figure 9, curves 1a and 2a). This is in qualitative agreement with the experimental data of Tanaka *et al* [54] and Gaudry *et al* [55], where the frequency of the peak shifts towards the lower-frequency side with decreasing size. Mercier *et al* [11] have found that the resonance frequencies in spherical Co–Ni and Fe–Co–Ni particles depend on the magnetic particle size. When the particle size decreases, an overall shift of the bands toward high frequencies is observed. This would correspond to the case of $J_s > J_b$ (figure 9, curves 1b and 2b). Unfortunately, there are not so many experimental data on the spin excitations in nanoparticles.

The damping increases with decreasing particle size for the two cases $J_s < J_b$ and $J_s > J_b$ (figure 10), which is in agreement with many experimental data [1, 2, 14, 18, 54, 56]. The inverse damping is proportional to the relaxation time. Since the relaxation time of magnetic nanoparticles can be changed by changing the size of the nanoparticles or using different kinds of materials, magnetic nanoparticles have been (and will be in the future) a very useful tool in different kinds of applications, from biomedical [57, 58] to data storage systems.

The above mentioned results are obtained without external magnetic field H. Applying a magnetic field with a specific frequency and amplitude it is possible for the magnetic nanoparticles to absorb energy, resulting in an increase in the local temperature around the nanoparticle system. This is used in *in vivo* applications in medicine to destroy tumour cells. In such cases, magnetic nanoparticles with materials with Curie temperatures at approximately 42 °C (the temperature where the tumour cells are destroyed) are preferred. For these materials, overheating problems can be avoided. The particle system will then work as a thermostat. In other applications where local heating is required, magnetic particles can also be used. In all of these cases, it is important to really understand the magnetic properties of the particle systems. Taking into account the influence of an external magnetic field we have calculated numerically

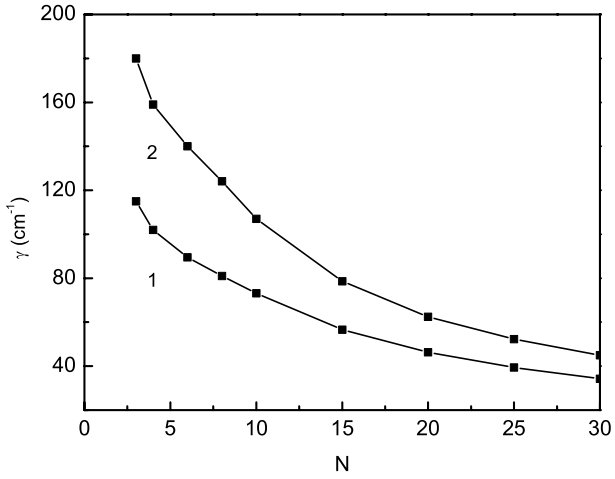

Figure 10. Particle size dependence of the spin excitation damping γ for $D_s = D_b$, $T = 800$ K and different J_s-values: (1) $J_s = 0.2J_b$ and (2) $J_s = 2J_b$.

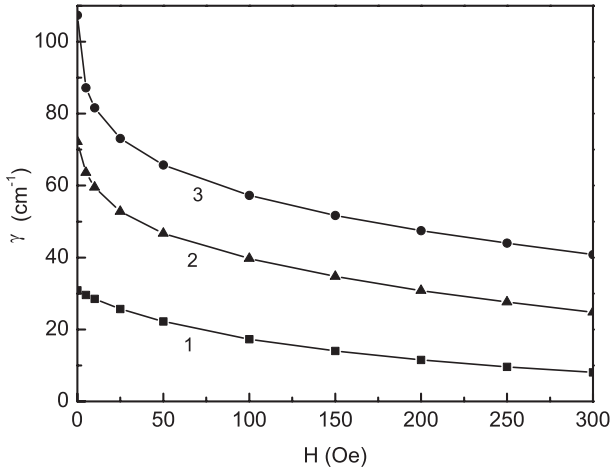

Figure 11. Magnetic field dependence of the damping γ for $J_s = 0.5J_b$, $D_s = 2D_b$, $N = 7$ and different temperature T-values: (1) $T = 300$, (2) 600 and (3) 800 K.

the magnetization M, the Curie temperature T_C, the spin excitations E and their damping γ. We obtain that M, T_C and E increase with increasing external magnetic field H, whereas the damping of the spin excitations γ decreases with H (figure 11). So, decreasing of particle size and magnetic field leads to large damping effects. There is some competition between the particle size N and the intensity of the magnetic field H. The magnetization, the phase transition temperature and the spin excitation energy can decrease with increasing particle size N for the case $J_s > J_b$ and increase with increasing applied magnetic field H.

4. Conclusions

Using the Heisenberg model and the method of real-space Green's functions we have calculated the magnetization, the spin-excitation energy and the damping of small spherical ferromagnetic

particles. The temperature and size dependence is discussed. It must be noted that for the case $J_s > J_b$, for example $J_s = 2\ J_b$, and strong surface anisotropy, for example $D_s/D_b = 2$, the magnetization is larger compared to the bulk and the curve in the size dependence of the magnetization $M(N)$ has a maximum at low particle size, $n = 4$ (figure 8, curves 1 and 3). We obtain the temperature, anisotropy and particle size dependence of the spin-excitation energy E and the damping γ. The spin-excitation energy (figure 5, curves 1a and 1b) (and analogously the magnetization) decreases with increasing surface anisotropy values D_s, whereas the damping increases with increasing D_s (figure 5, curves 2a and 2b). There is some competition between the influence of J_s, which enhances the magnetization M and the spin excitation energy E, and of D_s, which reduces them. Whereas the spin-excitation energy can increase or decrease, the damping always increases strongly with lowering of particle size. The influence of an external magnetic field is discussed, too. It increases the spin excitation energy and decreases the damping. The theoretical results are in good qualitative agreement with the experimental data of ferromagnetic small particles.

References

[1] Goya G F, Berquo T S, Fonseca F C and Morales M P 2003 *J. Appl. Phys.* **94** 3520
[2] Liu F, Li T and Zheng H 2004 *Phys. Lett.* A **323** 305
[3] Sanchez R D, Ramos C A, Rivas J, Vaqueiro P and Lopez-Quintela M A 2004 *Physica* B **354** 104
[4] Zhang Z, Chen X, Zhang X and Shi C 2006 *Solid State Commun.* **139** 403
[5] Chen J P, Sorensen C M, Klabunde K J and Hadjipanayis G C 1995 *Phys. Rev.* B **51** 11527
[6] Alves C R, Aquino R, Depeyrot J, Cotta T A P, Sousa M H, Tourinho F A, Rechenberg H R and Goya G F 2006 *J. Appl. Phys.* **99** 08M905
[7] Hori H, Yamamoto Y, Iwamoto T, Miura T, Teranishi T and Miyake M 2004 *Phys. Rev.* B **69** 174411
[8] Lefmann K, Bodker F, Klausen S N, Hansen M F, Clausen K N, Lindgard P A and Morup S 2001 *Europhys. Lett.* **54** 526
[9] Klausen S N, Lefmann K, Lindgard P A, Kuhn L T, Bahl C R H, Frandsen C, Morup S, Roessli B, Cavadini N and Niedermayer C 2004 *Phys. Rev.* B **70** 214411
[10] Kodama R H 1999 *J. Magn. Magn. Mater.* **200** 359
[11] Mercier D, Levy J-C S, Viau G, Fievet-Vincent F, Fievet F, Toneguzzo P and Acher O 2000 *Phys. Rev.* B **62** 532
[12] Ferchmin A R 2003 *Phys. Status Solidi* a **196** 13
[13] Roy S, Dubenko I, Edorh D D and Ali N 2004 *J. Appl. Phys.* **96** 1202
[14] Respaud M, Goiran M, Broto J M, Yang F H, Ould Ely T, Amiens C and Chaudret B 1999 *Phys. Rev.* B **59** R3934
[15] Gueron S, Deshmukh M M, Myers E B and Ralph D C 1999 *Phys. Rev. Lett.* **83** 4148
[16] Deshmukh M M, Kleff S, Gueron S, Bonet E, Pasupathy A N, von Delft J and Ralph D C 2001 *Phys. Rev. Lett.* **87** 226801
[17] Hsu K H, Wu J H, Huang Y Y, Wang L Y, Lee H Y and Lin J G 2005 *J. Appl. Phys.* **97** 114322
[18] Sharma V K and Baiker A 1981 *J. Chem. Phys.* **75** 5596
[19] Kuhn L T, Lefmann K, Bahl C R H, Ancona S N, Lindgard P-A, Frandsen C, Madsen D E and Morup S 2006 *Phys. Rev.* B **74** 184406
[20] Hendriksen P V, Linderoth S and Lindgard P A 1993 *J. Phys.: Condens. Matter* **5** 5675
Hendriksen P V, Linderoth S and Lindgard P A 1993 *Phys. Rev.* B **48** 7259
[21] Canali C M and MacDonald A H 2000 *Phys. Rev. Lett.* **85** 5623
[22] Ferchmin A R and Puszkarski H 2001 *J. Appl. Phys.* **90** 5335
[23] Cehovin A, Canali C M and MacDonald A H 2003 *Phys. Rev.* B **68** 14423
[24] Arias R, Chu P and Mills D L 2005 *Phys. Rev.* B **71** 224410
[25] Morup S and Hansen B R 2005 *Phys. Rev.* B **72** 024418
[26] Garanin D A, Kachkachi H and Reynaud L 2006 *Preprint* cond-mat/0609074
[27] Shilov V P, Bacri J-C, Gazeau F, Perzynski R and Raikher Yu L 1999 *J. Appl. Phys.* **85** 6642
[28] Shilov V P, Raikher Yu L, Bacri J-C, Gazeau F and Perzynski R 1999 *Phys. Rev.* B **60** 11902
[29] Usadel K D 2006 *Phys. Rev.* B **73** 212405
[30] Tserkovnikov Yu 1971 *Theor. Math. Phys.* **7** 250
[31] Pishko V V, Gnatchenko S L, Tsapenko V V, Kodama R H and Makhlouf S A 2003 *J. Appl. Phys.* **93** 7382
[32] Winkler E, Zysler R D, Mansilla M V and Fiorani D 2005 *Phys. Rev.* B **72** 132409

[33] Sousa E C, Alves C R, Aquino R, Sousa M H, Goya G F, Rechenberg H R, Tourinho F A and Depeyrot J 2005 *J. Magn. Magn. Mater.* **289** 118
[34] Morais P C, Lara M C F L, Tronconi A L, Tourinho F A, Pereira A R and Pelegrini R 1996 *J. Appl. Phys.* **79** 7931
[35] Morais P C, Tronconi A L, Tourinho F A and Pelegrini F 1997 *Solid State Commun.* **101** 693
[36] Bakuzis A F, Morais P C and Pelegrini F 1999 *J. Appl. Phys.* **85** 7480
[37] Rubinstein M, Kodama R H and Makhlouf S A 2001 *J. Magn. Magn. Mater.* **234** 289
[38] Koseoglu Y, Yildiz F, Salazar-Alvarez G, Toprak M and Muhammed M 2005 *Phys. Status Solidi* b **242** 1712
[39] De Biasi E, Ramos C A, Zysler R D and Romero H 2004 *Physica* B **354** 286
[40] Wada S, Hoshina T, Yasuno H, Ohishi M, Kakemoto H, Tsurumi T and Yashima M 2005 *Advances in Electronic Ceramic Materials* vol 26, ed D Zhu and W M Kriven (New York: Wiley) p 89
[41] Ishikawa K, yoshikawa K and Okada N 1988 *Phys. Rev.* B **37** 5852
Fu D, Suzuki H and Isjikawa K 2000 *Phys. Rev.* B **62** 3125
[42] Yu T, Shen Z X, Toh W S, Xue J M and Wang J 2003 *J. Appl. Phys.* **94** 618
[43] Neel L and Hebd C R 1961 *Seances Acad. Sci.* **252** 4075
[44] Morup S and Frandsen C 2004 *Phys. Rev. Lett.* **92** 217201
[45] Barbara B and Chudnovsky E M 1990 *Phys. Lett.* A **145** 205
[46] Kodama R H and Berkowitz A E 1999 *Phys. Rev.* B **59** 6321
[47] Respaud M, Broto J M, Rakoto H, Fert A R, Thomas L, Barbara B, Verelst M, Snoeck E, Lecante P, Mosset A, Osuna J, Ould Ely T, Amiens C, Chaudret B, Xie Y and Blackmann J A 2004 *J. Phys.: Condens. Matter* **16** 3163
[48] Chunder S, Kumar S, Krishnamurthy A, Srivastava B K and Aswal V K 2003 *Pramana J. Phys.* **61** 617
[49] Fernandez C de J, Mattei G, Maurizio C, Cattaruzza E, Padovani S, Battaglin G, Gonella F, D'Acapito F and Mazzoldi P 2005 *J. Magn. Magn. Mater.* **290/291** 187
[50] Bakuzis A F and Morais P C 2001 *J. Magn. Magn. Mater.* **226–230** 1924
[51] Morais P C, Lara M C F L and Tourinho F A 1998 *J. Magn. Res.* **134** 180
[52] Sanchez R D, Rivas J, Vaqueiro P, Lopez-Quintela M A and Caeiro D 2002 *J. Magn. Magn. Mater.* **247** 92
[53] Maaz K, Mumtaz A, Hasanain S K and Ceylon A 2007 *J. Magn. Magn. Mater.* **308** 289
[54] Tanaka A, Onari S and Arai T 1992 *Phys. Rev.* B **45** 6587
[55] Gaudry M, Lerme J, Cottancin E, Pellarin M, Vialle J-L, Broyer1 M, Prevel B, Treilleux M and Melinon P 2001 *Phys. Rev.* B **64** 085407
[56] Ladizhansky V and Vega S 2000 *J. Phys. Chem.* B **104** 5237
[57] Guedes M H A, Sadeghiani N, Peixoto D L G, Coelho J P, Barbosa L S, Azvedo R B, Kueckelhaus S, Da Silva M de F, Morais P C and Lacava Z G M 2005 *J. Magn. Magn. Mater.* **293** 283
[58] Xu Y H, Bai J and Wang J-P 2007 *J. Magn. Magn. Mater.* **311** 131